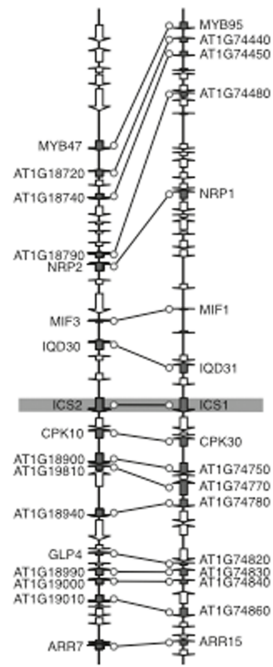
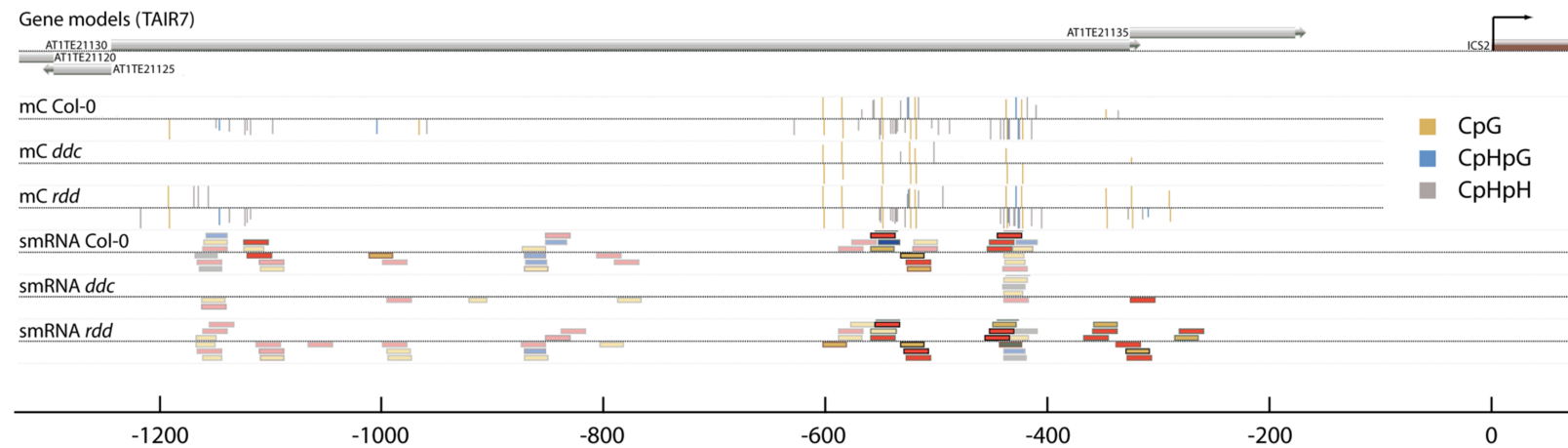
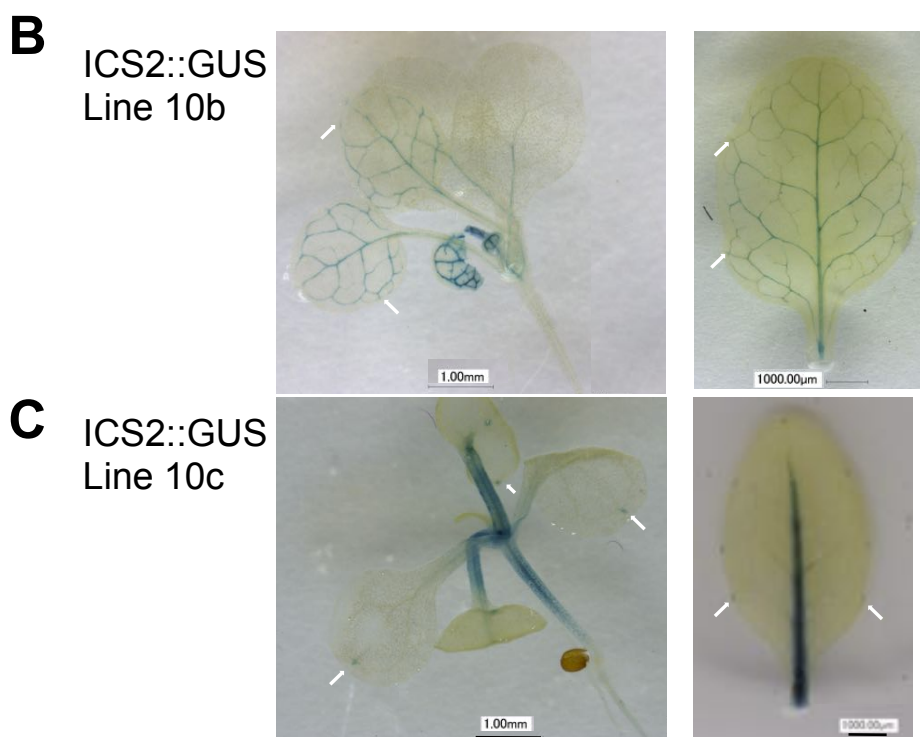
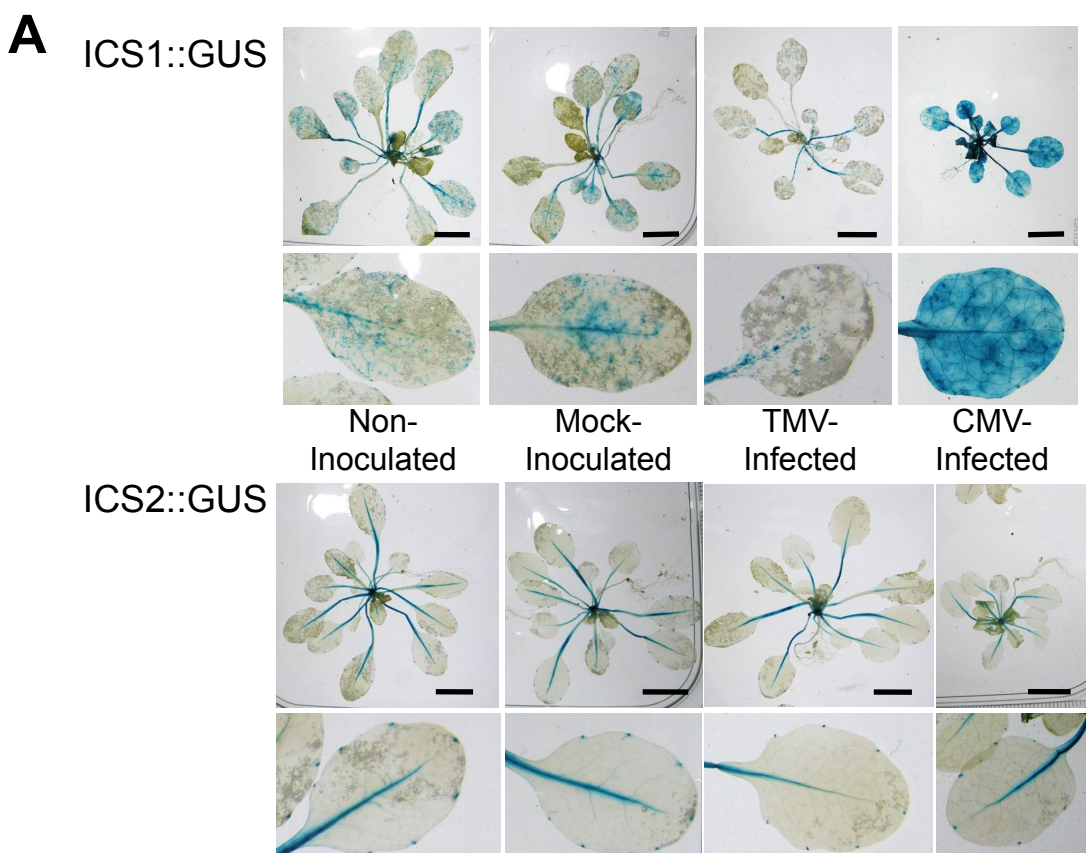
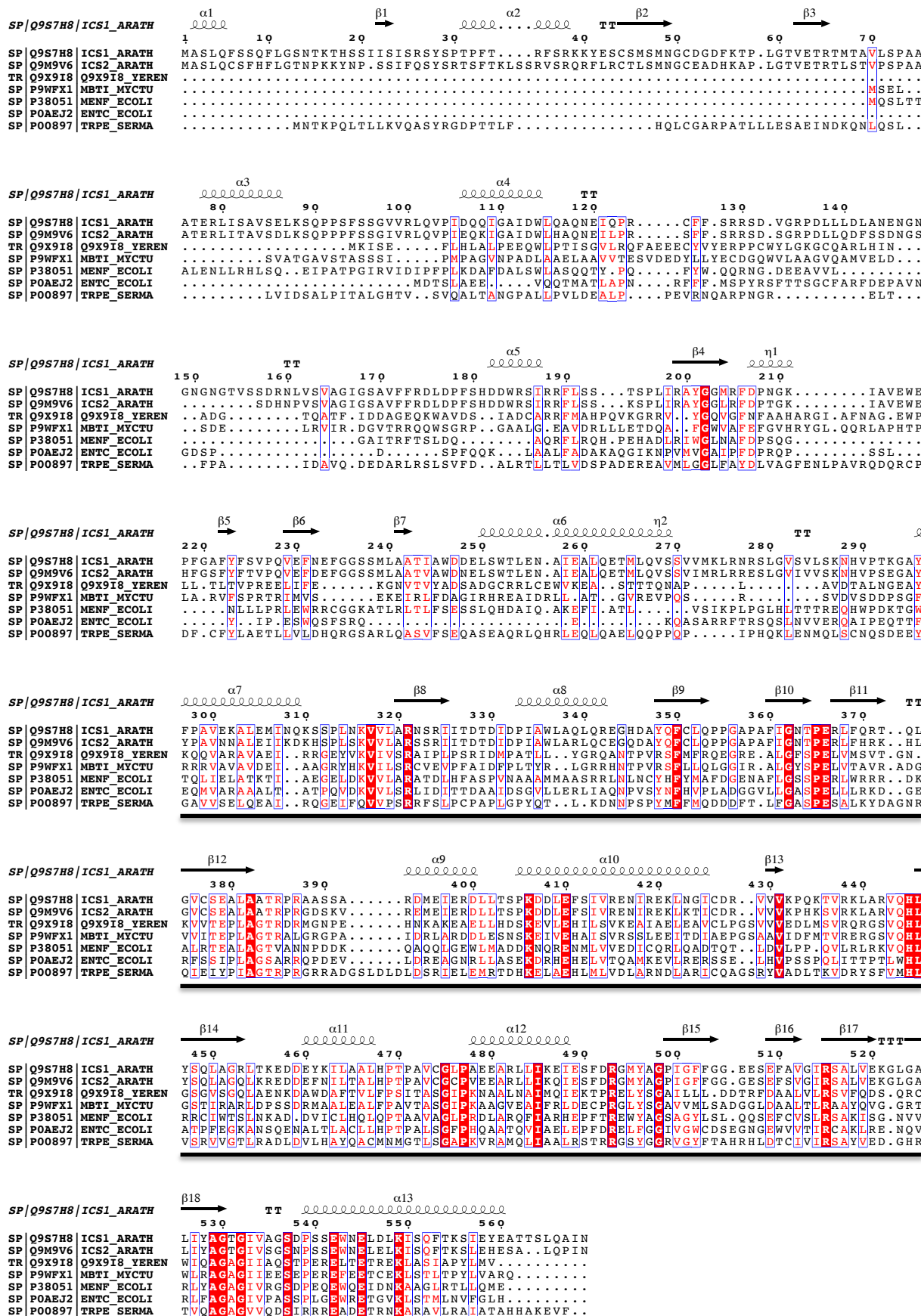


A**B**

Supplementary Figure S1. Genomic context of *AtICS1* and *AtICS2* genes and putative *AtICS2* promoter methylation sites. **A.** The two regions of chromosome 1 that contain the genes *AtICS1* (AT1G74710) and *ATICS2* (AT1g18870) are shown, indicated by shading. **B.** Whole genome bisulphite sequencing data (Lister et al., 2008) was inspected for regions of DNA methylation in the *ATICS2* promoter. The upper track shows cytosine residues methylated (mC) in DNA from wild-type (Col-0) at either CpG, CpHpG or CpHpH contexts (where H = A or C or T, but not G). The next track shows the sequencing information for a mutant unable to establish DNA methylation (*ddc* = *drm1 drm2 cmt3*). This triple mutant has lesions in two *DOMAINS REARRANGED METHYLASE (DRM)* genes, which condition RNA-directed DNA methylation, and *CYTOSINE METHYLTRANSFERASE (CMT)*, which methylates at CpHpG contexts. The third track shows DNA methylation in a triple mutant unable to demethylate (*rdd* = *ros1 dml2 dml3*) with lesions in two *DEMETER-LIKE (DML)* genes and one *REPRESSOR OF SILENCING (ROS)* gene, which are 5-mC DNA glycosylases. The lowest three tracks represent small RNA (smRNA) sequencing information obtained from wild type Col-0 and *ddc* and *rdd* mutants. Colouring of smRNA reads represent the length of the smRNA: 21-mers in blue, 23-mers in orange, 24-mers in red and smRNAs mapping to multiple locations are shown faded. The top of the map shows TAIR 7 gene models, including likely locations of transposable elements (TEs). The region -1500 to -1200, which was included in the construction of *ICS* promoter-GUS reporter constructs, did not contain any additional features of interest. Panel B was produced using AnnoJ Beta v1.1 (<http://www.annoj.org>) and the Arabidopsis epigenome map data previously described by Lister and colleagues (2008).



Supplementary Figure S2. Expression of *AtICS* promoter- β -glucuronidase reporter gene constructs in planta. A. Infection of transgenic Arabidopsis plants harbouring AtICS1::GUS fusions with cucumber mosaic virus (CMV) stimulates β -glucuronidase (GUS) activity throughout leaf tissue (indicated by blue staining). Neither mock-inoculation nor infection with tobacco mosaic virus (TMV) cause any increase in GUS activity beyond the basal levels (most apparent in vascular tissues). In contrast, GUS activity in plants harbouring an AtICS2::GUS transgene is unaffected by CMV infection. Inspection of GUS activity in unstressed leaves and plants of two AtICS2::GUS-transgenic lines, 10b (B) and 10c (C), indicates that AtICS2 promoter activity is most apparent in the vasculature with expression evident in the vicinity of hydathodes (arrowed). GUS activity was detected by vacuum infiltration of plants/tissues with 5-bromo-4-chloro-3-indolyl- β -D-glucuronic acid, overnight incubation at 37 °C, and destaining in 70% v/v ethanol [12,28].



Supplementary Figure S3 Structure-based alignment of amino acid sequences of AtICSs with other chorismate-utilising enzymes. Sequence alignment was performed using CLUSTAL W (Thompson et al., 1994) and aligned to the modeled ICS1 structure using ESPript (Gouet et al., 1999). Alpha (α) and eta (η , 3_{10}) helices are indicated by coils, beta (β) sheets with arrows and turns with a T. The approximate location of the chorismate binding domain is shown by a continuous black line (Wildermuth et al., 2001). ICS1_ARATH, *Arabidopsis thaliana* isochorismate synthase 1; ICS2_ARATH, *A. thaliana* isochorismate synthase2; Q9X9I8_YEREN, *Yersinia enterocolitica* salicylate synthase; MBTI_MYCTU, *M. tuberculosis* salicylate synthase; MENF_ECOLI, *Escherichia coli* menaquinone-specific isochorismate synthase; ENTC_ECOLI, *E. coli* enterobactin-specific isochorismate synthase; TRPE_SERMA, *Serratia marcescens* anthranilate synthase.

Supplementary Figure S4

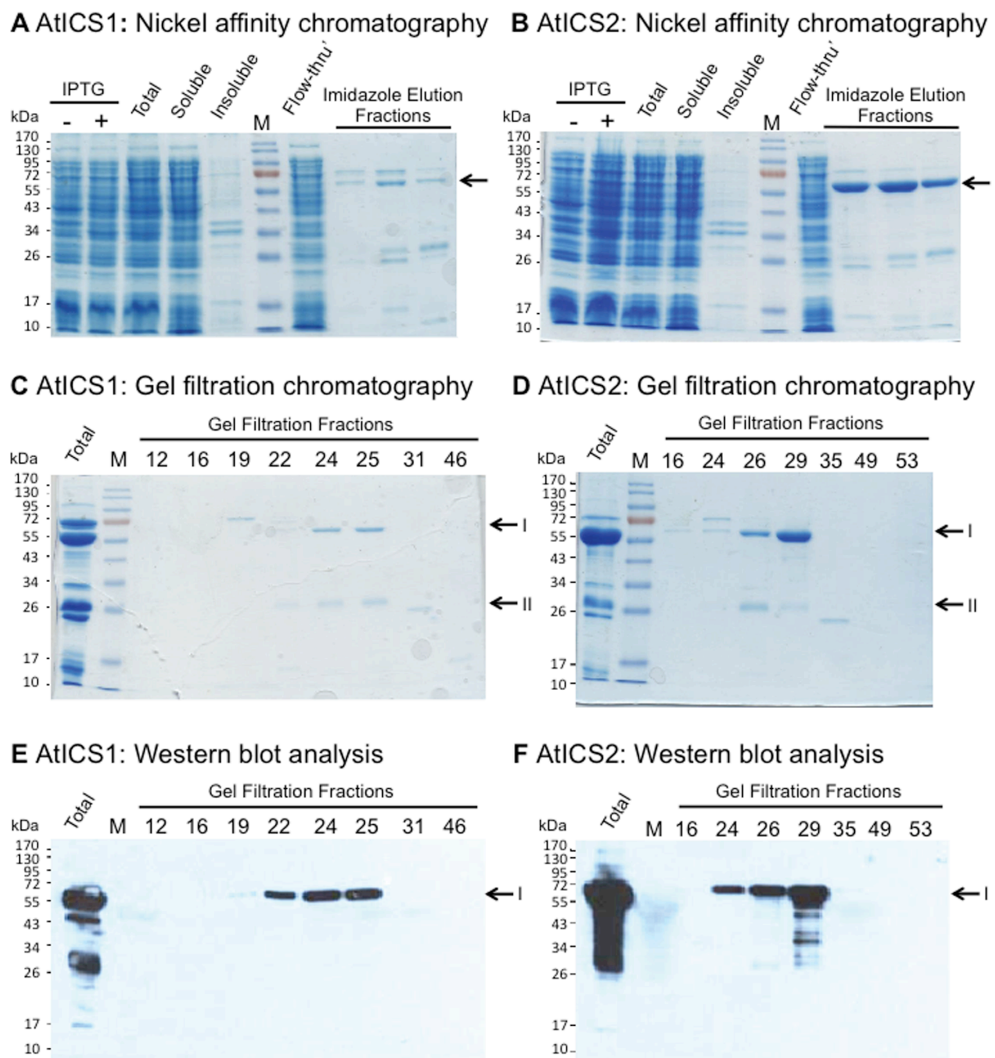
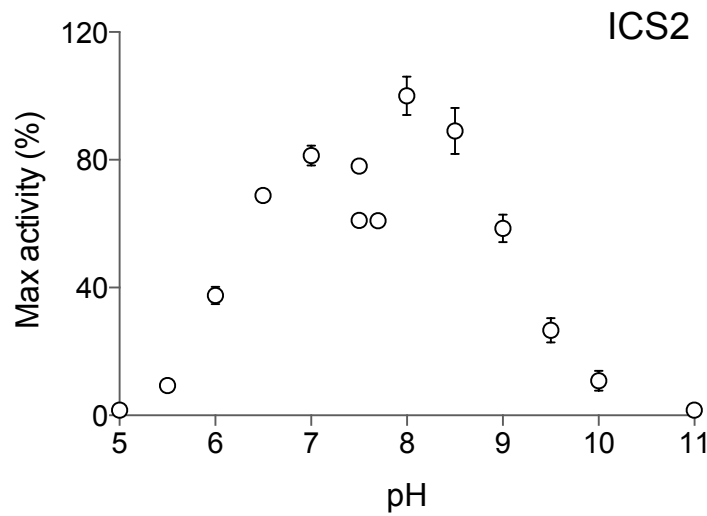
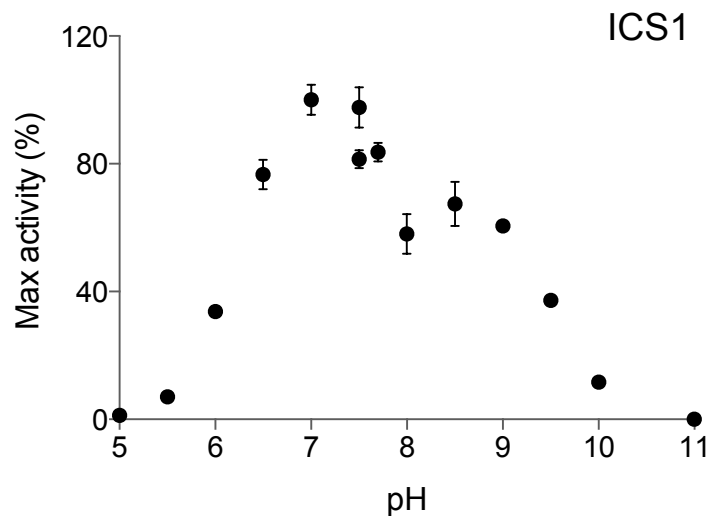


Figure S4. Expression of His₆-AtICS1 and His₆-AtICS2 fusion proteins in *E. coli* and their purification by nickel nitrilo tri-acetic acid (Ni-NTA) affinity chromatography and gel filtration. SDS polyacrylamide gel electrophoresis (SDS-PAGE) of cell lysates of *E. coli* transformed with vectors harbouring inserts encoding His₆-AtICS1 (A) and His₆-AtICS2 (B) fusion proteins. In A and B lysates from cells incubated or not incubated with isopropyl β-D-thiogalactopyranoside (IPTG) to induce fusion protein expression are indicated by + or -, respectively. In A and B, lane numbers 3-5 show, respectively, polypeptides present in an IPTG-induced cell lysate and after centrifugal fractionation into its soluble and insoluble components. Lanes 7 in A and B are loaded with polypeptides present in the soluble fraction of the cell lysates that were not bound by an Ni-NTA affinity chromatography column (Flow-thru') and subsequent lanes were loaded with proteins eluted by washing the column with a gradient of 20-500 mM imidazole. The positions of the predicted 60 kDa bands predicted for AtICS1 (A) and AtICS2 (B) are indicated with arrows. Affinity chromatography fractions containing the predicted 60 kDa ICS bands were pooled (indicated by Total) and further purified by gel filtration (C, D). Gel filtration

fractions containing the predicted 60 kDa band for AtICS1 (C) and AtICS2 (D) were identified. These bands are indicated with arrows labelled I. These fractions also contained lower mass polypeptides (arrows labelled II) that may have been contaminants or breakdown products of the ICS polypeptides. Western immunoblot analysis of the gel filtration fractions using anti-His₆ antibodies confirmed that the 60 kDa bands indicated by I were the authentic His₆-AtICS1 (E) and His6-AtICS2 (F) fusion proteins. Polypeptide bands in SDS-PAGE gels A-D were visualized by staining with Coomassie Brilliant Blue R-250. Binding of anti-His₆ in the western blots E and F was detected using a secondary antibody tagged with horseradish peroxidase and visualized on X-ray film after application of a chemiluminescent substrate. Lanes M were loaded with pre-stained protein markers and marker sizes in kDa are indicated to the left of each panel.



Supplementary Figure S5 Effect of pH on recombinant AtICS1 and AtICS2. Activity was measured with coupled online fluorimetric assays. Buffers used to maintain different pH values are detailed in Materials & Methods.